Chemical Shifts

DOI: 10.1002/anie.200905390

Direct Assessment of Electron Delocalization Using NMR Chemical Shifts[**]

Stephan N. Steinmann, Daniel F. Jana, Judy I.-C. Wu, Paul von R. Schleyer, Yirong Mo, and Clémence Corminboeuf[*]

Dedicated to Prof. Dr. Werner Kutzelnigg

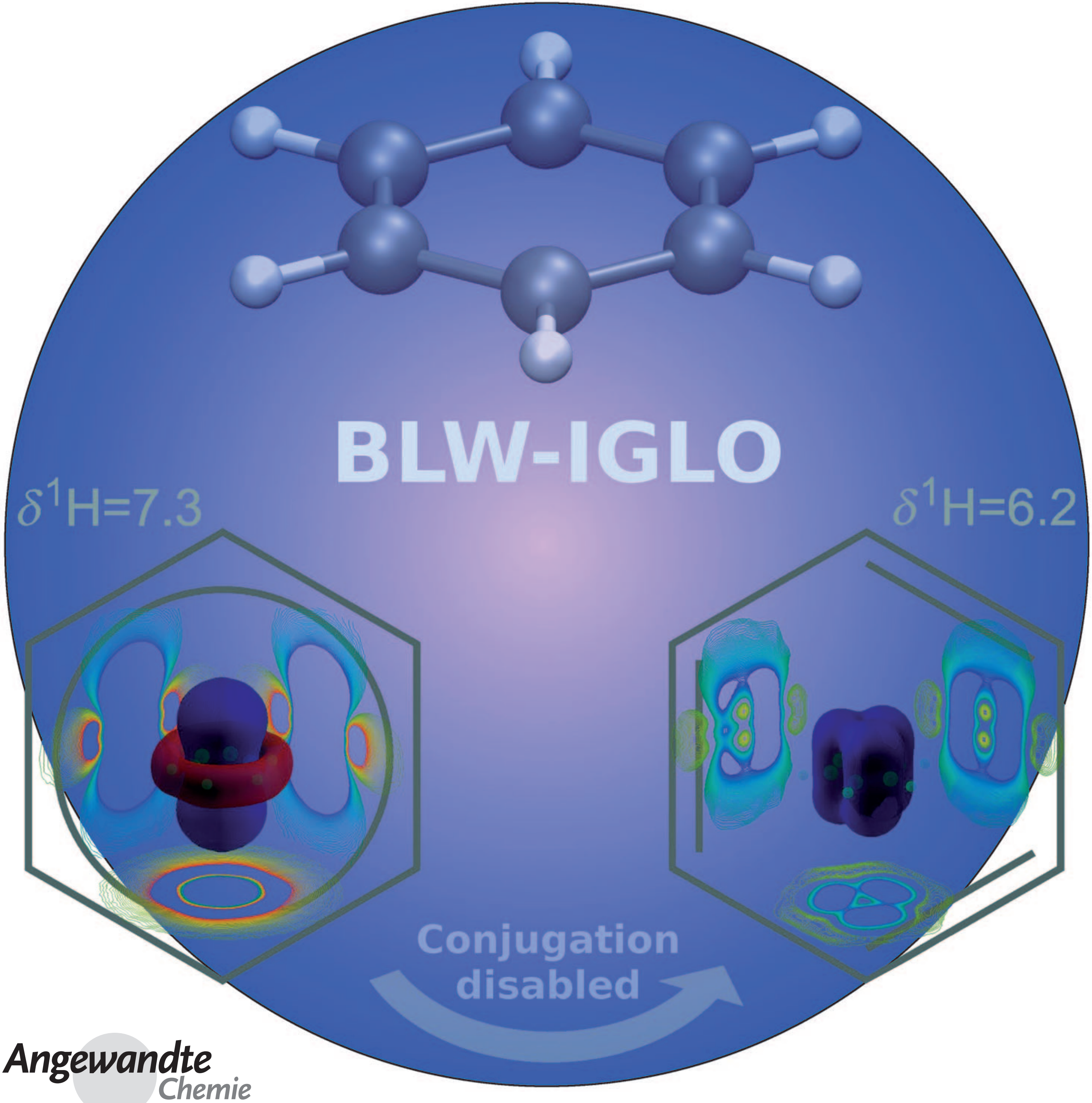

Proton chemical shifts in NMR spectroscopy have long been employed as primary experimental indicators of aromaticity in unsaturated organic rings. Thus, the benzene proton chemical shift $\delta(^1\mathrm{H}) = 7.3$ ppm is 1.6 ppm downfield from the $\delta = 5.6$–5.8 ppm range of the $\delta(^1\mathrm{H})$ of the olefinic protons in cyclohexene, 1,3-cyclohexadiene, and 1,4-cyclohexadiene.[1] As such deshielding is attributed to the induced diatropic ring currents of aromatic molecules, the induced paramagnetic ring currents of antiaromatic species should result in upfield $\delta(^1\mathrm{H})$ values.[2] However, the ^{1}H chemical shift of cyclobutadiene ($\delta = 5.8$ ppm)[1] is in the olefinic region and is almost the same as that of cyclobutene ($\delta = 6.0$ ppm).[3–5] This discrepancy is especially puzzling since the paratropicity of cyclobutadiene is well established.[6–9]

We now introduce the BLW-IGLO method, a quantum chemical approach that not only solves the cyclobutadiene mystery fully but also enables the direct assessment of π-electron delocalization effects on the NMR chemical shifts of polycyclic conjugated and hyperconjugated systems generally. Our computational strategy combines block-localized wavefunction (BLW) scheme developed by Mo et al.[10–12] with Kutzelnigg's IGLO methodology[13] to analyze the magnetic properties of model reference species with "chemically non-interacting" (disabled) double bonds.

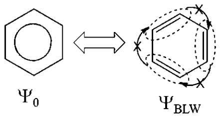

RE=E(Ψ_0)-E(Ψ_{BLW})

Scheme 1. Schematic depiction of a block-localized wavefunction. RE = resonance energy.

The BLW scheme[10–12] constructs and optimizes a block-localized wavefunction self-consistently to represent a specific resonance structure (i.e., a diabatic state), which can serve as a localized reference for comparison with the fully delocalized wavefunction energy (Scheme 1). This comparison evaluates the effect of electron delocalization on molecular energetics and geometries. In practice, the N electrons and M primitive orbitals are partitioned into k blocks. Each localized orbital is expanded in terms of the primitive orbitals only in its own block. The molecular orbitals (MOs) of a given block are mutually orthogonal, while the orbitals of different blocks have finite overlap. As an example, the wavefunction of hypothetical 1,3,5-cyclohexatriene, where the double bonds resemble those in ethylene, is given in Equation (1):

$$\Psi(4\mathrm{BLW}) = \hat{A}\left\{\Phi^{2\pi}_{\mathrm{C_1C_2}}\Phi^{2\pi}_{\mathrm{C_3C_4}}\Phi^{2\pi}_{\mathrm{C_5C_6}}\sigma\right\} \tag{1}$$

where $\Phi^{2\pi}_{\mathrm{C_1C_2}}$ denotes the occupied $\mathrm{C_1C_2}$ π molecular orbital, σ represents all the σ MOs, and $\hat{A}$ is the antisymmetrizer.

The combined BLW-IGLO method presented herein enables the analysis of the effect of electron delocalization on NMR chemical shifts and related magnetic properties. Unlike standard localized molecular orbitals (LMOs), the sets of BLW-DFT orbitals used in the IGLO computation have no residual delocalization tails. In other words, the interactions between occupied and virtual LMOs are quenched in the BLW-IGLO computations, producing the desired effect. Illustrative applications of this exciting BLW extension clarify "magnetic anomalies" (e.g. unexpected shielding or deshielding effects) of prototype molecules.[14]

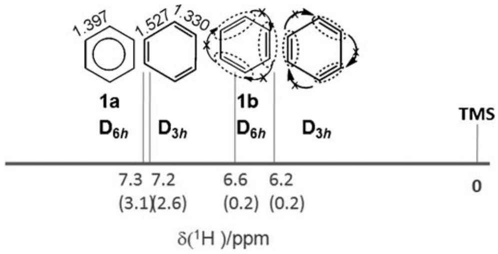

Figure 1. (BLW)-IGLO-PW91/IGLO-III isotropic NMR $\delta(^1\mathrm{H})$ chemical shifts for **1a** and **1b** (the π contribution to the out-of-plane shielding tensor components $\delta^{\pi}_{\perp}$ are given in parentheses) referenced to the experimental benzene proton chemical shift ($\delta = 7.27$).[1] Geometries were optimized at B3LYP/6-31G(d) for D_{6h} **1a** and **1b** and at BLW-B3LYP/6-31G(d) (fully optimized with the BLW constraints) for D_{3h} **1a** and **1b**. Bond lengths are in Å. Blocked double bonds are circled.

The geometric distortion of the D_{6h} symmetry of benzene (**1a**), for example, to an enforced D_{3h} 1,3,5-cyclohexatriene-like geometry has little effect on the proton chemical shift[15] (only $\delta = 0.1$ ppm, Figure 1, left) and only decreases the out-of-plane tensor component of the nucleus-independent chemical shift, the NICS(0)$_{\pi zz}$ value,[7,16,17] moderately from −36.3 to −28.2 (Figure 2). In sharp contrast, the "electronic" BLW distortion has far larger consequences. Eliminating the π conjugation by blocking all three π orbitals in D_{3h} **1b** (Figure 1 and Figure 2) reduces $\delta(^1\mathrm{H})$ to $\delta = 6.2$ ppm (the non-aromatic vinyl hydrogen region) and NICS(0)$_{\pi zz}$ to zero. Imposing a D_{6h} geometry on **1b** (but still with blocked π orbitals) increases both values only modestly (Figure 1 and Figure 2). As D_{6h} **1b** retains the benzene geometry, but has no conjugation, its non-aromatic vinyl hydrogen atoms ($\delta(^1\mathrm{H}) = 6.6$ ppm) are the ideal "non-aromatic" reference for **1a**. Blocking only a single π double bond as in **1c** (Figure S1,

---

[*] S. N. Steinmann, D. F. Jana, Prof. Dr. C. Corminboeuf
Institut des sciences et ingénierie chimiques
Ecole Polytechnique Fédérale de Lausanne, EPFL SB ISIC LCMD
1015 Lausanne (Switzerland)
Fax: (+41) 21-693-9700
E-mail: clemence.corminboeuf@epfl.ch
J. I.-C. Wu, Prof. Dr. P. v. R. Schleyer
Department of Chemistry, University of Georgia (USA)
Prof. Dr. Y. Mo
Department of Chemistry, Western Michigan University (USA)

[**] The Sandoz family foundation, the Swiss NSF Grant 200021_121577/1, and EPFL are acknowledged for financial support.

Supporting information for this article is available on the WWW under http://dx.doi.org/10.1002/anie.200905390.

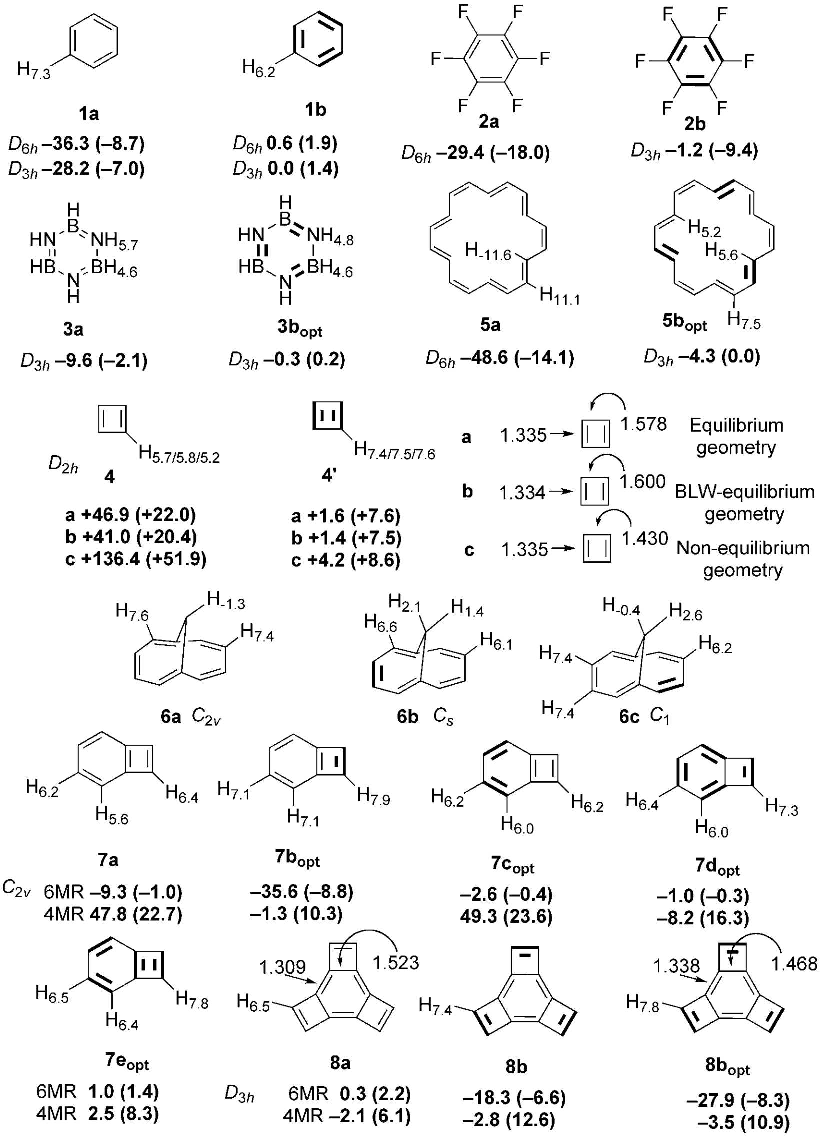

Figure 2. (BLW)-IGLO-PW91/IGLO-III isotropic NMR $\delta(^1H)$ chemical shifts referenced to the experimental benzene proton chemical shift ($\delta = 7.27$ ppm)[1] employing B3LYP/6-31G(d) geometries (BLW indicated as **opt**). Blocked double bonds are indicated in bold. $\text{NICS}(0)_{\pi zz}/(\text{NICS}(0)_{\text{isotropic}})$ values were computed at the individual ring centers. Owing to the nonplanarity of the π system, the **6b** geometry was not optimized with BLW. More details are given in the Supporting Information.

Supporting Information) also disables the π ring current completely. Thus, the "vinyl" protons on the blocked double bond resonate at $\delta = 6.3$ ppm, while those of remaining butadiene moiety ($\delta(^1H) = 6.6$ and 6.7 ppm) are deshielded by the conjugated double bonds but not by the "extra" ring current contributions.

As both π electronic structures and chemical shifts are anisotropic properties, their relationship depends on the Cartesian axis directions (x, y, z) as represented by the tensor components δ_{xx}, δ_{yy}, and δ_{zz}. The conventional isotropic chemical shift is the average of these three tensor components. The out-of-plane component of a planar molecule (δ^{π}_{zz} by convention; denoted here as $\delta^{\pi}_{\perp}$, with "π" indicating that only the π-electron contributions are considered) reflects the magnetic response of a molecule toward a magnetic field applied perpendicularly to the plane and is related to the current density.[16,18] As a proof of concept, the $\delta = 1.1$ ppm upfield shift ($\delta = 7.3$ (**1a**) to 6.2 ppm (**1b**), Figure 1 and 2) arising from the absence of a ring current in **1b** and **1c**, is given solely by the contribution of the out-of-plane component ($\delta^{\pi}_{\perp} = 3.1$ ppm, see Figure 1) of the proton chemical shielding tensor to the isotropic chemical shift ($\delta^{\pi}_{\text{iso}} = \delta^{\pi}_{\perp}/3 \rightarrow -3.1/3 = -1$ ppm).[18,19]

The generally contrasting magnetic responses between benzene **1a** and the localized cyclohexatriene structure **1b** are illustrated in more detail by the magnetic shielding function isosurface shown in Figure 3. The isovalues correspond to the out-of-plane component of the shielding tensor[20,21] for the delocalized (i.e., $\sigma^{\pi}_{\perp}(R)_{1a}$) and localized (i.e., $\sigma^{\pi}_{\perp}(R)_{1b}$) structures. Their difference ($\Delta\sigma^{\pi}_{\perp}(R)_1$) reflects the magnetic effects arising solely from π-electron delocalization. Note that the plots of the shielding isosurfaces are equivalent to maps of spatial distribution of $\text{NICS}_{\pi zz}$ or induced magnetic field (i.e., B^{π}_{z} values).[22] At the ring center, $\sigma^{\pi}_{\perp}(R_0) = -\text{NICS}(0)_{\pi zz}$.

Three features evident in Figure 3 differentiate D_{6h} benzene **1a** from localized **1b**. The benzene protons (**1a**) are in the deshielding region (red), while those of **1b** are not. The pronounced localization of the three π orbitals in **1b** contrasts with the shape of the isolines encompassing the benzene framework in **1a**. As is typical for systems lacking global ring currents, the π magnetic shielding is negligible at the **1b** center (see $\text{NICS}(0)_{\pi zz}$ in Figure 2) and is not as long-range as **1a** (see $\Delta\sigma^{\pi}_{\perp}(R)_1$ plot in Figure 3). The marginal difference between $\Delta\sigma^{\pi}_{\perp}(R)$ of hexafluorobenzene (**2**) and benzene (**1a**) provides a direct comparison and indicates that both have nearly the same degree of electron delocalization.[23] While ring current effects dominate the magnetic properties characterizing benzene and other strongly aromatic species, the much weaker ring current in borazine **3a** results in an imperceptible deshielding zone in $\Delta\sigma^{(\pi)}_{\perp}(R)_3$ (only noticeable at smaller isosurface values, see Figure S2 in the Supporting Information) and much shorter-range shielding inside the ring. However, even the modest shielding of borazine ($\text{NICS}(0)_{\pi zz} = -9.6$) in **3a** is eliminated by the block localization ($\text{NICS}(0)_{\pi zz} = -0.3$) in **3b**$_{\textbf{opt}}$. The borazine results corroborate the presence of only a weak diatropic ring current[24–26] and do not support the original "inorganic benzene" description.[27]

The BLW-IGLO effects on cyclobutadiene (CBD; **4a**) are opposite to those of benzene. The paratropic regions inside

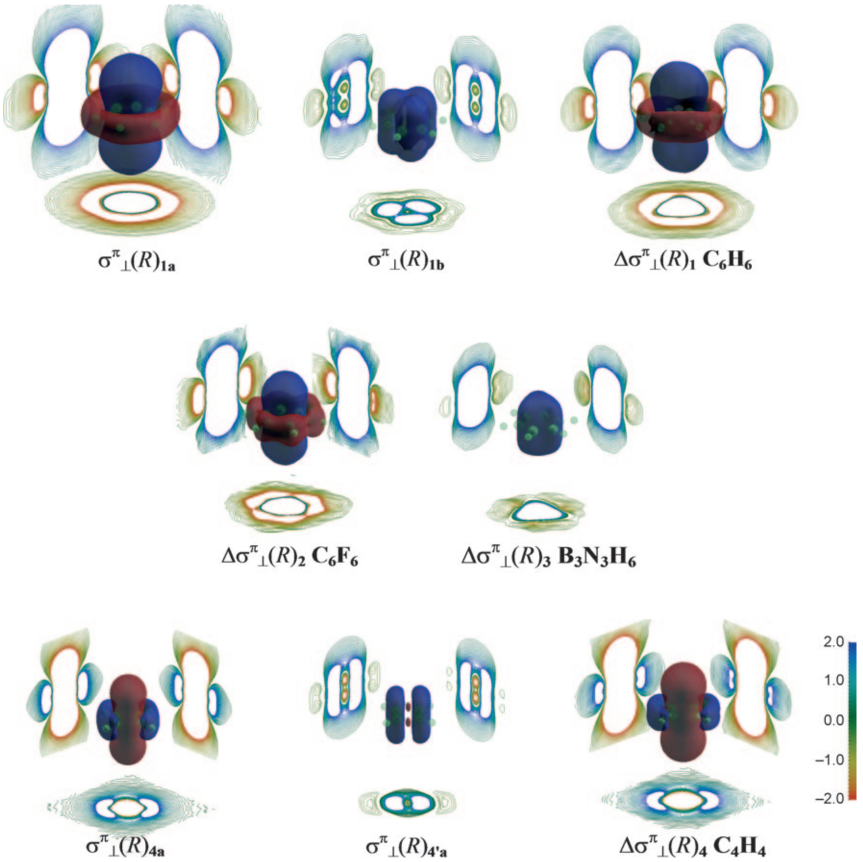

Figure 3. Isosurface plots (2 ppm value) of the out-of-plane shielding tensor components, and the shielding differences $\Delta\sigma^{\pi}{}_{\perp}(R)$ between the fully delocalized (e.g. $\sigma^{\pi}{}_{\perp}(R)_{1a}$ for **1a**, D_{6h}) and block-localized (e.g. $\sigma^{\pi}{}_{\perp}(R)_{1b}$ for **1b** D_{6h}) structures of benzene (**1**), hexafluorobenzene (**2**), borazine (**3**), and cyclobutadiene (**4**). Shielding/deshielding zones are indicated in blue/red. Magnetic shielding computations at (BLW)-IGLO-PW91/IGLO-III employed standard (i.e. non-BLW) B3LYP-6-31G* geometries. The hydrogen and heavy atoms locations are indicated by small and large light green spheres, respectively.

the CBD ring ($\sigma^{\pi}{}_{\perp}(R)_{4a}$) vanish when the two π bonds are blocked (in $\sigma^{\pi}{}_{\perp}(R)_{4'a}$). Also, the $\sigma^{\pi}{}_{\perp}(R)_{4a}$ and $\Delta\sigma^{\pi}{}_{\perp}(R)_{4}$ plots of cyclobutadiene are barely distinguishable, as the paratropic global ring current fully dominates. BLW-IGLO also resolves the puzzling anomaly of olefin-like ^{1}H chemical shift of cyclobutadiene.[3,4] As noted earlier,[5] the $\delta(^1H)$ of CBD (experimental $\delta = 5.76$ ppm; computed 5.7 ppm) is only slightly upfield ($\delta = 0.3$ ppm) from the vinyl $\delta(^1H)$ of cyclobutene ($\delta = 6.0$ ppm).[1] This situation suggests, at least superficially, that the paratropic ring current[2] of CBD is much weaker than the diatropic ring current of benzene (see above). However, the existence of a strong paratropic current in CBD has been confirmed by other theoretical studies.[6,8,9] The reason for this apparent discrepancy is clarified by the $\delta(^1H) = 7.5$ ppm computed for the atropic **4′b** ($\mathrm{NICS}(0)_{\pi zz} = 1.4$). The $\delta(^1H)$ value $\delta = 7.5$ ppm is an ideal non-antiaromatic vinyl hydrogen benchmark for CBD, owing to the non-interacting π bonds but intact cyclobutadiene framework of **4′b**. Dimethylenecyclobutene is a much better reference than cyclobutene for probing the paratropic ring current in cyclobutadiene. The computed $\delta(^1H)$ values for the ring −CH= protons in dimethylenecyclobutene (7.65 ppm) are close to the $\delta = 7.5$ ppm of **4′b**. Note that going from **4b** (BLW equilibrium geometry) to the hypothetical **4c** (closer to a square) increases the isotropic NICS values and the upfield ^{1}H shifts owing to the small gap between the highest occupied and lowest unoccupied MOs (HOMO–LUMO gap).[8] The BLW-IGLO values (**4′a**, **b**, and **c**) are, in contrast, barely affected by the geometry change.

Much larger direct ring current effects are illustrated by the ^{1}H chemical shifts of [18]-annulene (**5**; computed in D_{6h} symmetry[28]) and 1,6-methano[10]annulene (**6**). The large (ca. 20 ppm) difference between $\delta(^1H)$ of the inner and outer protons of **5a** decreases to a $\delta = 3$ ppm difference in **5b** when the π delocalization is “disabled”. Similarly, the annihilation of the π ring current reduces the $\mathrm{NICS}(0)_{\pi zz}$ from −48.6 in **5a** to −4.3 in **5b$_{opt}$**. The methylene protons of **6b** are shifted 3 ppm downfield (on average) compared to **6a**. An interesting example is the unambiguous presence of a homoaromatic benzene moiety in **6c**.

Another proof of concept is provided by the BLW-IGLO analysis of the mutual cancellation of paratropic and especially diatropic ring currents engendered by the fusion of the six- and four-membered rings (6MR and 4MR)[29,30] in benzocyclobutadiene (**7a**). The shielding at the 6MR center is reduced markedly ($\mathrm{NICS}(0)_{\pi zz} = -9.3$) as compared to −36.3 for benzene. Also, all the protons in **7a** resonate in the olefinic $\delta = 5.6$–6.4 ppm range. Localizing the two outer π orbitals of the 6MR (as in **7c**) has very little effect on the chemical shifts of both the 6MR and 4MR protons of **7c** (compare to **7a**). This finding confirms the absence of a delocalized sextet in benzocyclobutadiene. In contrast, the 4MR moiety in **7a** ($\mathrm{NICS}(0)_{\pi zz} = +47.8$) is as paratropic as cyclobutadiene **4a** ($\mathrm{NICS}(0)_{\pi zz} = +46.9$). Localizing the outer 4MR π orbital (as in **7b$_{opt}$**) restores the benzene-like proton chemical shift ($\delta = 7.1$ ppm) and the $\mathrm{NICS}_{\pi zz}$ value (−35.6) for the 6MR but annihilates the paratropic current of the 4MR ($\mathrm{NICS}_{\pi zz} = -1.3$) almost completely.

In contrast to **7**, the electron localization of tricyclobutabenzene (**8**) results from both geometric distortion and mutual cancellation of the 4MR paratropic and 6MR diatropic ring current. Unlike D_{3h} benzene (**1a**), which is only constrained geometrically and has a modestly decreased $\mathrm{NICS}(0)_{\pi zz}$ value (−28.2), the central ring of **8a** ($\mathrm{NICS}(0)_{\pi zz} = 0.3$) resembles the electronically constrained cyclohexatriene (D_{3h} **1b**, $\mathrm{NICS}_{\pi zz} = 0.0$; Figure 2). When the outer 4MR double bonds are localized, **8b** reclaims over half ($\mathrm{NICS}(0)_{\pi zz} = -18.3$) of the π ring current of D_{3h} **1a**. When the geometry is relaxed (as in **8b$_{opt}$**), another $\delta = 10$ ppm

($\mathrm{NICS(0)}_{\pi zz} = -27.9$) is regained; this value matches the difference of D_{3h} and D_{6h} benzene. Akin to CBD, the 4MR $\delta(^1\mathrm{H})$ in **7a** and **8a** ($\delta(^1\mathrm{H}) = 6.4$ and 6.5 ppm) are shifted upfield when compared to the "localized" reference data lying above the usual olefinic ^{1}H chemical shift region (e.g. $\delta = 7.9$ in **7b**$_{\mathbf{opt}}$, 7.8 ppm in **8b**$_{\mathbf{opt}}$).

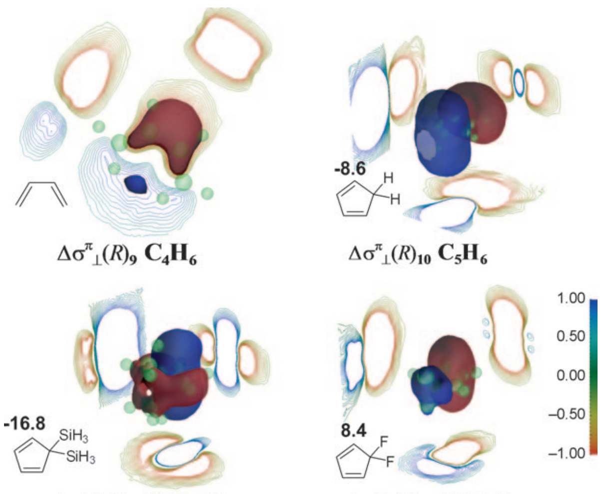

$\Delta\sigma^{\pi}_{\perp}(R)_9$ C_4H_6 $\Delta\sigma^{\pi}_{\perp}(R)_{10}$ C_5H_6

$\Delta\sigma^{\pi}_{\perp}(R)_{11}$ $C_5H_{10}Si_2$ $\Delta\sigma^{\pi}_{\perp}(R)_{12}$ $C_5H_4F_2$

Figure 4. Isosurface plots (1 ppm value) of the out-of-plane shielding tensor component difference: $\Delta\sigma^{\pi}_{\perp}(R)$ for **9–12** at the same levels as given in Figure 3. Standard $\mathrm{NICS(0)}_{\pi zz}$ values are in bold. Note the similarities between $\Delta\sigma^{\pi}_{\perp}(R)_{11}$ and $\Delta\sigma^{\pi}_{\perp}(R)_1$ for benzene as well as between $\Delta\sigma^{\pi}_{\perp}(R)_{12}$ and $\Delta\sigma^{\pi}_{\perp}(R)_4$ for cyclobutadiene. See the Supporting Information for details.

Much weaker magnetic currents, for example those induced by simple π conjugation, can also be analyzed by BLW-IGLO. The shielding function difference plots ($\Delta\sigma^{\pi}_{\perp}(R)$) identify the π-delocalization effects of such systems (Figure 4) effectively. Since the magnetic shielding function of conjugated compounds is not dominated by the π-electron delocalization, the individual $\sigma^{\pi}_{\perp}(R)_{\mathrm{delocalized/localized}}$ maps are more difficult to interpret than their difference (see the Supporting Information). The smaller and more local (de)shielding zones of the $\Delta\sigma^{\pi}_{\perp}(R)$ plots of **9–12** reflect the weaker effects of their electron delocalization compared to **1–4**. Despite the negligible effect of localization on the olefinic proton chemical shifts in *syn*-butadiene (**9**), π delocalization across all the sp^2-hybridized carbon atoms results in a stronger deshielding zone in the vicinity of the carbon–carbon single bond. The similar pattern characterizing the closely related 1,3-cyclopentadiene (**10**) is somewhat more pronounced. Localization has an additional but opposite effect around the methylene group. The overall result is due to the hyperconjugative interaction with the methylene group, which serves as a weak two-π-electron donor.[31] Despite the negative $\mathrm{NICS(0)}_{\pi zz}$ value (−8.6) at the center of **10a**, its shielding pattern ($\Delta\sigma^{\pi}_{\perp}(R)_{10}$) does not indicate the presence of a ring current.[32] Clearly, the magnetic properties of π-hyperconjugated 5MRs are more tunable than those of compounds exhibiting strong ring currents. The greater π-donor ability of the *gem*-disilyl group in 5,5-disilylcyclopentadiene (**11**)[32] changes the magnetic pattern markedly; its $\mathrm{NICS(0)}_{\pi zz}$ value of −16.8 is half that of benzene, and $\Delta\sigma^{\pi}_{\perp}(R)_{11}$ resembles $\Delta\sigma^{\pi}_{\perp}(R)_1$ to some extent, with a large shielding zone inside the ring and an incomplete deshielding loop outside. Conversely, $\Delta\sigma^{\pi}_{\perp}(R)_{12}$, representing the π-electron delocalization in the difluoro-substituted analogue (**12**), resembles a 4-π-electron ring, with long-range character inside evocative of the $\Delta\sigma^{\pi}_{\perp}(R)_4$ of cyclobutadiene. Nevertheless, the breached shielding region of **12** and deshielding region of **11** outside the ring suggest that substituted cyclopentadienes may be better described as having "augmented cyclic conjugation" than a uniform "ring current".

The BLW-IGLO method enables direct quantitative evaluation of π-electron delocalization effects on chemical shift values. It provides otherwise unperturbed computational NMR spectral references for the olefinic $\delta(^1\mathrm{H})$ values of unsaturated organic rings. For instance, comparisons with the $\delta(^1\mathrm{H})$ of ideal "block-localized" reference structures ($\delta = 7.3$–7.9 ppm) reveal the expected upfield ^{1}H chemical shift of cyclobutadiene and its derivatives ($\delta = 5.7$–6.5 ppm). Imposed geometrical constraints (e.g. C–C bond-length alternation) have only modest effects on the magnetic properties of cyclic conjugated molecules (e.g. delocalized D_{3h} benzene, **1a**), but electronic constraints can eliminate their dia- or paratropicity completely (**1b**). The BLW-IGLO method also is useful for probing the magnetic responses of individual rings (e.g. in benzo-fused cyclobutadienes) and clearly differentiates borderline cyclic (hyper)conjugated compounds from those exhibiting global ring currents (on the basis of their $\Delta\sigma^{\pi}_{\perp}(R)$ plots).

Further studies involving the direct probing and tuning of π-electron delocalization effects on the properties of materials and biomolecules are underway.

Experimental Section

Electronic structure computations employed a modified version of GAMESS-US (release 2008)[33,34] interfaced with the BLW-module.[10–12] The code was adapted to output the energies and eigenvectors for the complete set of (block localized) occupied and virtual molecular orbitals. This information is then read by a modified version of the deMon-MASTER code[35] that computes the NMR parameters by numerical integration for both the delocalized and BLW structures.

Unless otherwise stated, the non-BLW-PW91/IGLO-III wavefunction computations of the magnetic properties employed standard B3LYP/6-31G(d) geometries. Both standard and localized (i.e. BLW constrained) B3LYP/6-31G(d) geometries were used for the BLW-PW91/IGLO-III wavefunction computations. The (BLW)-PW91/IGLO-III orbitals based on the IGLO method as implemented in the deMon-MASTER package were used to compute proton chemical shifts, magnetic shielding function,[21] and the nucleus-independent chemical shifts (i.e. NICS-based indices).[6,7] Isotropic NMR ^{1}H chemical shifts are referenced to the experimental benzene proton chemical shift ($\delta = 7.27$ ppm).[1] The Pipek–Mezey[36] MO localization and the chemical shift dissection were based on the σ/π symmetry. Chemical shifts were improved by the LOC1 ad hoc correction for virtual orbitals.[37] The graphical representations of the magnetic shielding function isosurfaces employed OpenDX 4.4.4.[38]

Received: September 25, 2009
Revised: October 20, 2009

Keywords: aromaticity · conjugation · electron delocalization · NMR spectroscopy · ring current

[1] H. Günther in *NMR-Spektroskopie: Eine Einführung in die Protonenresonanz-Spektroskopie und ihre Anwendungen in der Chemie*, Georg Thieme, Stuttgart, **1983**.
[2] J. A. Pople, K. G. Untch, *J. Am. Chem. Soc.* **1966**, *88*, 4811.
[3] As deduced from Cram's measurement of CBD and C_6H_6 in a hemicarcerand: D. J. Cram, M. E. Tanner, R. Thomas, *Angew. Chem.* **1991**, *103*, 1048; *Angew. Chem. Int. Ed. Engl.* **1991**, *30*, 1024.
[4] The vinyl ^{1}H chemical shift ($\delta = 5.38$ ppm) of tri-*tert*-butylcyclobutadiene is given in T. Bally, S. Masamune, *Tetrahedron* **1980**, *36*, 343.
[5] M. Balci, M. L. McKee, P. v. R. Schleyer, *J. Phys. Chem. A* **2000**, *104*, 1246.
[6] P. v. R. Schleyer, C. Maerker, A. Dransfeld, H. J. Jiao, N. J. R. v. E. Hommes, *J. Am. Chem. Soc.* **1996**, *118*, 6317.
[7] Z. Chen, C. S. Wannere, C. Corminboeuf, R. Puchta, P. v. R. Schleyer, *Chem. Rev.* **2005**, *105*, 3842.
[8] C. van Wüllen, W. Kutzelnigg, *Chem. Phys. Lett.* **1993**, *205*, 563.
[9] T. Heine, R. Islas, G. Merino, *J. Chem. Comput.* **2006**, *28*, 302.
[10] Y. Mo, S. D. Peyerimhoff, *J. Chem. Phys.* **1998**, *109*, 1687.
[11] Y. Mo, J. Gao, S. D. Peyerimhoff, *J. Chem. Phys.* **2000**, *112*, 5530.
[12] Y. Mo, *J. Chem. Phys.* **2003**, *119*, 1300.
[13] W. Kutzelnigg, *Isr. J. Chem.* **1980**, *19*, 193.
[14] Other BLW-IGLO applications, including detailed analysis of the individual orbital contributions, will be reported in future work.
[15] U. Fleischer, W. Kutzelnigg, P. Lazzeretti, V. Muehlenkamp, *J. Am. Chem. Soc.* **1994**, *116*, 5298.
[16] C. Corminboeuf, T. Heine, G. Seifert, P. v. R. Schleyer, *Phys. Chem. Chem. Phys.* **2004**, *6*, 273.
[17] H. Fallah-Bagher-Shaidaei, C. S. Wannere, C. Corminboeuf, R. Puchta, P. v. R. Schleyer, *Org. Lett.* **2006**, *8*, 863.
[18] R. G. Viglione, R. Zanasi, P. Lazzeretti, *Org. Lett.* **2004**, *6*, 2265.
[19] C. S. Wannere, C. Corminboeuf, W. D. Allen, H. F. Schaefer III, P. v. R. Schleyer, *Org. Lett.* **2005**, *7*, 1457.
[20] Special Issue, *Chem. Rev.* **2005**, *105*, 10.
[21] T. Heine, C. Corminboeuf, G. Seifert, *Chem. Rev.* **2005**, *105*, 3889.
[22] G. Merino, T. Heine, G. Seifert, *Chem. Eur. J.* **2004**, *10*, 4367.
[23] J. I. Wu, F. G. Pühlhofer, P. v. R. Schleyer, R. Puchta, B. Kiran, M. Mauksch, N. J. R. v. E. Hommes, E. I. Alkorta, J. Elguero, *J. Phys. Chem. A* **2009**, *113*, 6789.
[24] P. v. R. Schleyer, H. Jiao, N. J. R. v. E. Hommes, V. G. Malkin, O. L. Malkina, *J. Am. Chem. Soc.* **1997**, *119*, 12669.
[25] E. Steiner, A. Soncini, P. W. Fowler, *J. Phys. Chem. A* **2006**, *110*, 12882.
[26] R. Islas, P. W. Chamorro, J. Robles, T. Heine, G. Merino, *Struct. Chem.* **2007**, *18*, 833.
[27] E. Wiberg, *Naturwissenschaften* **1948**, *35*, 182.
[28] C. S. Wannere, K. W. Sattelmeyer, H. F. Schaefer III, P. v. R. Schleyer, *Angew. Chem.* **2004**, *116*, 4296; *Angew. Chem. Int. Ed.* **2004**, *43*, 4200.
[29] A. Soncini, R. W. A. Havenith, P. W. Fowler, L. W. Jenneskens, E. Steiner, *J. Org. Chem.* **2002**, *67*, 4753.
[30] A. Stanger, *J. Am. Chem. Soc.* **1991**, *113*, 8277.
[31] R. S. Mulliken, *J. Chem. Phys.* **1939**, *7*, 339.
[32] L. Nyulászi, P. v. R. Schleyer, *J. Am. Chem. Soc.* **1999**, *121*, 6872.
[33] M. W. Schmidt, K. K. Baldridge, J. A. Boatz, S. T. Elbert, M. S. Gordon, J. J. Jensen, S. Koseki, N. Matsunaga, K. A. Nguyen, S. Su, T. L. Windus, M. Dupuis, J. A. Montgomery, *J. Comput. Chem.* **1993**, *14*, 1347.
[34] M. S. Gordon, M. W. Schmidt in *Theory and Applications of Computational Chemistry: The First Forty Years* (Eds.: C. E. Dykstra, G. Frenking, K. S. Kim, G. E. Scuseria), Elsevier, Amsterdam, **2005**.
[35] Modified version of deMon-Master, see: V. G. Malkin, O. L. Malkina, M. E. Casida, D. R. Salahub, *J. Am. Chem. Soc.* **1994**, *116*, 5898.
[36] J. Pipek, P. G. Mezey, *J. Chem. Phys.* **1989**, *90*, 4916.
[37] V. G. Malkin, O. L. Malkina, D. R. Salahub, *Chem. Phys. Lett.* **1993**, *204*, 87.
[38] OpenDX 4.4.4, http://www.opendx.org.